

Faraday Discussions

Accepted Manuscript



This manuscript will be presented and discussed at a forthcoming Faraday Discussion meeting. All delegates can contribute to the discussion which will be included in the final volume.

Register now to attend! Full details of all upcoming meetings: <http://rsc.li/fd-upcoming-meetings>



This is an *Accepted Manuscript*, which has been through the Royal Society of Chemistry peer review process and has been accepted for publication.

Accepted Manuscripts are published online shortly after acceptance, before technical editing, formatting and proof reading. Using this free service, authors can make their results available to the community, in citable form, before we publish the edited article. We will replace this *Accepted Manuscript* with the edited and formatted *Advance Article* as soon as it is available.

You can find more information about *Accepted Manuscripts* in the [Information for Authors](#).

Please note that technical editing may introduce minor changes to the text and/or graphics, which may alter content. The journal's standard [Terms & Conditions](#) and the [Ethical guidelines](#) still apply. In no event shall the Royal Society of Chemistry be held responsible for any errors or omissions in this *Accepted Manuscript* or any consequences arising from the use of any information it contains.



Journal Name

ARTICLE

Water oxidation catalysis upon evolution of molecular Co(III) cubanes in aqueous media

Andrea Genoni,^a Giuseppina La Ganga,^c Andrea Volpe,^a Fausto Puntoriero,^c Marilena Di Valentin,^a Marcella Bonchio,^a Mirco Natali^{b*} and Andrea Sartorel^{a*}

Received 00th January 20xx,
Accepted 00th January 20xx

DOI: 10.1039/x0xx00000x

www.rsc.org/

The increasing global energy demand has stimulated great, recent efforts in investigating new solutions for artificial photosynthesis, a potential source of clean and renewable solar fuels. In particular, according to the generally accepted modular approach, aimed at optimising separately the different compartments of the entire process, many studies have focused on the development of catalytic systems for water oxidation to oxygen. While in recent years there have been many reports on new catalytic systems, the mechanism and the active intermediates operating the catalysis have been less investigated. Well-defined, molecular catalysts, constituted by transition metals stabilised by a suitable ligand pool, could help in solving this aspect. However, in some cases molecular species have been shown to evolve to active metal oxides, that constitute the other side of this catalysis dichotomy. In this paper, we address the evolution of tetracobalt(III) cubanes, stabilised by a pyridine/acetate ligand pool, to active species that perform water oxidation to oxygen. Primary evolution of the cubane in aqueous solution is likely initiated by removal of an acetate bridge, opening the coordination sphere of the Cobalt centres. This Cobalt derivative, where the pristine ligands still impact on the reactivity, shows enhanced electron transfer rates to Ru(bpy)₃³⁺ (*hole scavenging*), within a photocatalytic cycle with Ru(bpy)₃²⁺ as the photosensitiser and S₂O₈²⁻ as the electron sink. A more accentuated evolution occurs under continuous irradiation, where Electron Paramagnetic Resonance (EPR) spectroscopy reveals the formation of Co(II) intermediates, likely contributing to the catalytic process that evolves oxygen. All together, these results confirm the relevant effect of molecular species, in particular in fostering the rate of the electron transfer processes involved in the light activated cycles, pivotal for the design of a photoactive device.

Introduction

In recent years, artificial photosynthesis (AP) has been the subject of intense investigation, due to its potential impact in the renewable energy sector.[1,2] Indeed, its final goal is to exploit sunlight to convert small molecules like water and carbon dioxide into solar fuels, such as hydrogen and methanol.[1,2] AP systems are generally described as a modular arrangement of key components enabling different functions such as light absorption, energy and electron transfer, and redox catalysis.[3] Optimisation of the functional modules is often carried out separately, before engineering the overall assembly. In particular, the development of catalytic systems enabling the redox processes under light

irradiation has achieved important results during the last decade.[4] Many efforts have especially focused on the oxidation of water to oxygen (eq. 1), which is plagued by thermodynamic issues (reduction potential for the O₂/H₂O couple is 1.23-0.059×pH V vs NHE) and kinetic barriers. This is due to the complexity of mechanism where four electrons and four protons are abstracted from two water molecules, while a new oxygen-oxygen bond is formed.[5-7]



As a consequence, in a relatively short timeframe there has been an explosion of scientific reports on this subject, mainly focused on the development of new water oxidation catalysts (WOCs) and on the optimization of their performance, while reaction mechanism and identification of active species have been less investigated.[8] In some cases, transition metal complexes claimed as molecular, water oxidation catalysts, were actually observed to undergo a major decomposition, in the harsh, oxidizing conditions required for the catalysis, leading to the formation of catalytically active metal oxide phases, being the actual operating species.[9-12] Therefore, the questions “what is the competent catalyst?” and “is it a molecular catalyst?” appear to be fundamental ones in this field; indeed, the great potential of molecular chemistry in fine-tuning

^a Department of Chemical Sciences, University of Padova and ITM-CNR, via Marzolo 1, 35131 Padova (Italy).

^b Dipartimento di Scienze Chimiche e Farmaceutiche, Università di Ferrara and Centro Interuniversitario per la Conversione Chimica dell'Energia Solare, sezione di Ferrara, Via Fossato di Mortara 17-19, 44121 Ferrara, Italy.

^c Dipartimento di Scienze Chimiche, Università di Messina and Centro Interuniversitario per la Conversione Chimica dell'Energia Solare, sezione di Messina, Via Sperone 31, 98166 Messina, Italy.

† Electronic Supplementary Information (ESI) available: synthetic procedures and characterisation spectra. See DOI: 10.1039/x0xx00000x

the properties and the activity of a catalyst, together with the possibility of identification of active intermediates and comprehension of reaction mechanism, often faces with stability issues of the molecule itself, and with the good activity of metal oxides, especially conceived in nanostructured forms.[9-12]

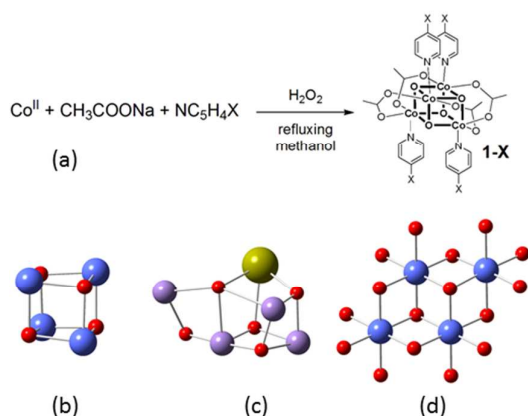


Figure 1. Schematic representation of the synthetic procedure for the tetracobalt(III) cubane **1-H** (a), and structural representation of the $\text{Co}_4^{\text{III}}\text{O}_4$ core (b), of the CaMn_4O_x oxygen evolving centre (c) and of a fragment of the heterogeneous CoPi catalyst (d). Colour code: blue: Cobalt; violet: Manganese; yellow: Calcium; red: Oxygen; blue: Nitrogen; gray: Carbon. Hydrogen atoms are omitted for clarity reasons.

One recent example deals with the tetracobalt(III) cubanes, with general formula $\text{Co}_4\text{O}_4(\text{OAc})_4(\text{X-py})_4$, hereafter **1-X**, where OAc = acetate and X-py = *p*-substituted pyridines ($\text{X} = \text{H}, \text{Me}, t\text{-Bu}, \text{OMe}, \text{COOMe}, \text{CN}, \text{Br}$), see figure 1a. The key motif of this class of compounds is the $\text{Co}(\text{III})_4\text{O}_4$ cubic core (figure 1b),[13] that was proposed as a structural model of the CaMn_4O_x oxygen evolving centre (figure 1c), operating in biological water oxidation.[14-15] More recently,[16-17] molecular cubanes were identified as models of the Cobalt phosphate/oxide catalyst (CoPi) developed by Kanan and Nocera in 2008 (figure 1d), a milestone discovery in the field of water oxidation electrocatalysis.[18-19]

The water oxidation activity of **1-H** was initially investigated by cyclic voltammetry experiments and under light assisted catalysis, in the presence of the well-known $\text{Ru}(\text{bpy})_3^{2+} / \text{S}_2\text{O}_8^{2-}$ sacrificial system ($\text{bpy} = 2,2'$ -bipyridine).[20-21] A significant effect of the substituent X in *para* position of the pyridines, on the redox potentials, on the kinetics of electron transfer within the light activated cycle, and on the rate and quantum yield for oxygen production, evidenced a decisive role of the ligand pools on the activity of the cubanes.[22] As a consequence, further studies were aimed at investigating the effect of the nuclearity of $\text{Co}(\text{III})$ -oxo bridged species on their activity,[23-24] while the activity of **1-H** in catalytic water oxidation was recently studied in a light activated system with a porphyrin as the photosensitizer,[25] and in a photoelectrochemical cell, where **1-H** was embedded in a Nafion membrane and supported onto a hematite ($\alpha\text{-Fe}_2\text{O}_3$) semiconductor.[26] Modification of the ligand pool, in particular introducing ethynyl moieties to the carboxylate groups lead to an

enhancement of the quantum yield of oxygen production in the light assisted cycle;[27] a cubane analog with $\text{Co}(\text{II})$ centres and a flexible 2-(hydroxymethyl)pyridine ligand was also proposed as a water oxidation catalyst.[28]

More recently, the water oxidation ability of the **1-X** species was severely questioned by Nocera et al.,[29] who attributed the major source of water oxidation catalysis to $\text{Co}(\text{II})$ impurities in the $\text{Co}(\text{III})$ cubanes, that likely evolve to the CoPi catalyst under application of anodic bias. Indeed, purification of the cubanes by silica chromatography lead to a major abatement of the anodic wave due to catalytic water oxidation, previously observed for the non-purified cubane. Consistently, the activity of the purified cubane was found to drop also in combination with the $\text{Ru}(\text{bpy})_3^{2+} / \text{S}_2\text{O}_8^{2-}$ light activated system, in buffered water at neutral pH. The residual activity of the cubane (ca 1/5 with respect to the non-purified batch) was attributed to a specific effect of the strongly oxidizing sulfate radical ($\text{SO}_4^{\cdot-}$, E^0 ca 2.4-3.4 V vs NHE)[30-33], which is formed within the sacrificial cycle (*vide infra*), although the evolution of the pristine cubane structure and generation of high valent Co -based intermediates capable of water oxidation was not excluded.[29]

In this paper, we have addressed the evolution of the $\text{Co}(\text{III})$ -cubane species in aqueous solution, where dissociation of an acetate bridge opening the coordination sphere of the Co_4O_4 core, is recognised as the first event of the cubane rearrangement, leading to the formation of a water oxidation catalyst. The steady building-up of this competent WOC is traced under dark electrocatalytic conditions and in a photoactivated cycle by monitoring the photoinduced electron transfer rate to $\text{Ru}(\text{bpy})_3^{3+}$. This latter turns out to be enhanced by ca 40 times with respect to the pristine cubane, and not ascribable to $\text{Co}(\text{II})$ aquo-ion, which is silent within the flash photolysis time-frame. Evolution of the $\text{Co}(\text{III})$ -cubane under continuous irradiation within the $\text{Ru}(\text{bpy})_3^{2+} / \text{S}_2\text{O}_8^{2-}$ cycle is also addressed by Electron Paramagnetic Resonance (EPR) Spectroscopy, revealing the formation of a $\text{Co}(\text{II})$ derivative, likely involved in the oxygenic cycle.

Results and discussion

Synthesis and purification of 1-X

Synthesis of **1-X** was performed according to the literature procedure,[13] by refluxing $\text{Co}(\text{II})$ ions (introduced as the hexahydrate nitrate salt) in methanol in the presence of acetate (2 eq.) and pyridine (1 eq.), followed by addition of hydrogen peroxide (figure 1). The crude, olive-green compounds are isolated by extraction and anhydrification in dichloromethane, and then purified by silica chromatography ($\text{CH}_2\text{Cl}_2:\text{CH}_3\text{OH}$ 95:5 eluent, see Experimental Section). As reported by Nocera et al.,[29] this procedure is mandatory to purify the **1-X** species from $\text{Co}(\text{II})$ by-products, that are not eluted and remain at the top of the silica column. The identity and purity of the isolated compounds were confirmed by combined elemental analysis, ^1H and ^{13}C -NMR, Electropray Ionisation Mass Spectrometry (ESI-MS) and UV-Visible spectroscopy techniques (see Supporting Information). However, the decisive proof for the purification of **1-X** from $\text{Co}(\text{II})$ species, comes from cyclic voltammetry (CV). Figure 2 reports the CV analysis for **1-H**, as a representative case, in 0.2 M phosphate

buffer, pH 7 (a), and in 0.2 M borate buffer, pH 8 (b). In both cases, under anodic scan, a reversible peak is observed at $E_{1/2} = 1.06$ V ($\Delta E = 80$ mV) vs Ag/AgCl, due to one electron oxidation of the $\text{Co}^{\text{III}}_4\text{O}_4$ core in **1-H** to a formal $\text{Co}^{\text{IV}}\text{Co}^{\text{III}}_3\text{O}_4$ mixed-valent intermediate, where the spin is actually localized over the four metals, thus displaying an average oxidation state $\text{Co}^{+3.25}$ (*vide infra*).[29] The absence of Co(II) impurities is confirmed by the lack of an intense anodic wave at higher potentials ($E > 1.2$ V vs Ag/AgCl),[20-21,29] which is diagnostic of the water oxidation process promoted by the Co(II) species.[29]

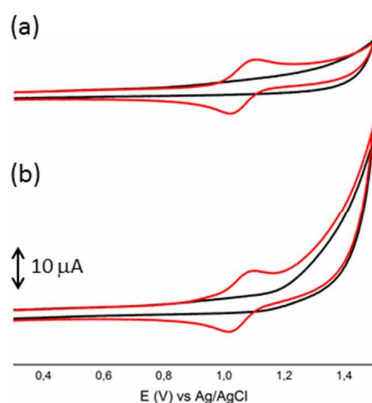


Figure 2. Cyclic voltammetry (CV) of 0.5 mM **1-H** (red traces; black traces represent the CV scans in the absence of **1-H**) in 0.2 M phosphate buffer, pH 7 (a) and 0.2 M borate buffer, pH 8 (b).

Evolution of **1-H** in aqueous solution

Inspection of figure 2 clearly indicates the absence of any electrocatalytic activity of purified **1-H** towards water oxidation.[29] However, a different behaviour was observed for solutions of the same **1-H** batch aged in water. In figure 3, the CV analysis of 0.5 mM **1-H** in 0.2 M borate buffer at different aging time is reported (**1-H** is aged in a 5 mM stock solution in milli-Q water, and then aliquots are diluted in 0.2 M borate buffer, where the CVs are immediately registered).

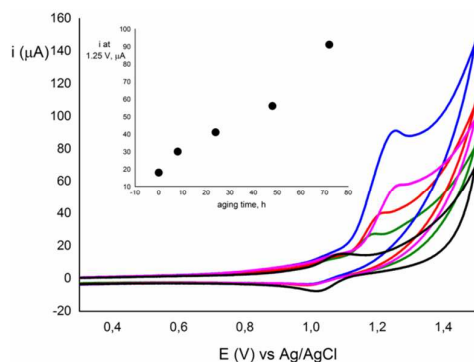


Figure 3. CVs of 0.5 mM **1-H** in 0.2 M borate buffer, pH 8, at different aging times (**1-H** is aged in water, at 5 mM concentration, and then aliquots of this stock solution are diluted in buffer); black trace: fresh solution, green trace: 8 h aging, red trace: 24 h aging,

pink trace: 48 h aging; blue trace: 72 h aging. The inset shows the plot of the intensity of the current at 1.25 V versus aging time.

Upon aging, the rising of an anodic wave at $E > 1.15$ V vs Ag/AgCl is observed, likely ascribable to water oxidation. Clearly, these results point to a steady accumulation of an active WOC upon incubation of the pristine cubane in aqueous solution up to 72 h (hereafter, we refer to this species as *active-Co*). Interestingly, the amount of *active-Co*, can be conveniently titrated with ethylenediaminetetraacetic acid (EDTA), which is known to bind Co(II) centers with a 1:1 stoichiometry, inhibiting water oxidation activity.[29] Indeed, EDTA addition to a solution of aged **1-H** leads to a complete abatement of the observed anodic water oxidation wave. Modification of the CV features resulting from **1-H** aged for 72 hours and upon titration with EDTA (aliquots of a 1 mM in 0.2 M borate buffer) are reported in figure 4a as a representative case, while the inset plots the current intensity of the anodic wave ($E = 1.25$ V vs Ag/AgCl) versus the EDTA/**1-H** ratio, levelling off at a value of 0.013 (corresponding to a 65 μM concentration in a stock 5 mM solution of **1-H**).

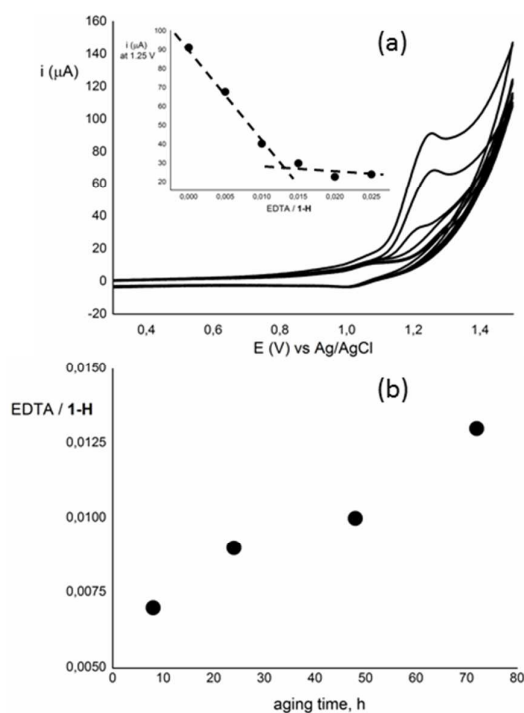


Figure 4. (a) Cyclic voltammetry of 0.5 mM **1-H** (aged 72 hours from a stock solution, 5 mM in water) in 0.2 M borate buffer, pH 8, upon addition of different aliquots of EDTA; the inset shows the plot of the intensity of the anodic wave at 1.25 V vs Ag/AgCl versus the $[\text{EDTA}]/[\text{1-H}]$ ratio. (b) Plot of the ratio EDTA/**1-H** at the equivalence point versus aging time.

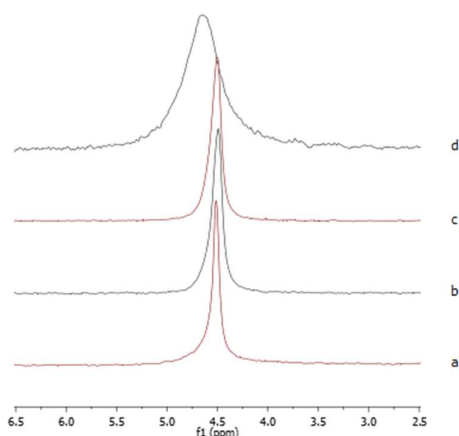


Figure 5. ^{31}P -NMR spectra of 0.1 M phosphate buffer, pH 8, with: (a) no species added; (b) 2.5 mM fresh **1-H**; (c) 2.5 mM aged **1-H**, from a 5 mM stock solution in water; (d) 25 μM Co(II) aquo ion.

To address the nature of *active-Co*, at first instance we checked if hydrolysis of **1-H** could be responsible for the release of Cobalt aquo ions in solution. In **1-H**, all the cobalt centres are in oxidation state III, and reduction of Co(III) to Co(II) is highly disfavoured, since the first wave under cathodic scan occurs at quite negative potentials of ca -700 mV vs Ag/AgCl, in 0.2 M borate buffer, pH 8. However, since the reduction potential of Co(III)/Co(II) aquo ions is 1.84 V vs Normal Hydrogen Electrode (i.e. Cobalt(III) aquo ions are strong oxidants) the release of Cobalt(III) aquo ions from **1-H** should be likely associated to reduction of Co(III) to Co(II) and parallel, partial oxidation of the organic ligands.[34,35] Therefore, we checked the presence of paramagnetic Co(II) aquo ions by means of ^{31}P NMR line broadening analysis.[29,36] The full width at half maximum (FWHM) has thus been recorded for the ^{31}P NMR signal resulting from a 0.1 M phosphate buffer solution (pH 8) under different conditions (Figure 5) and specifically: (a) in the absence of any additive; (b) with fresh **1-H** (2.5 mM); (c) with 48 h aged **1-H** (2.5 mM); (d) Co(II)(NO₃)₂ (25 μM , i.e., 1% amount with respect to the concentration of **1-H** in spectra c, in order to take into account the 1% of *active-Co*, formed upon 48 h aging). Inspection of figure 5 a-c spectra shows no broadening of the ^{31}P NMR signal (FWHM=12 Hz), which is instead significantly observed upon addition of Co(II) aquo ions (FWHM=50 Hz), Figure 5d. Therefore, the ^{31}P line broadening test speaks against the release of Co(II) aquo ions upon **1-H** aging in water, and that ligand pool of the cubane likely exerts some coordination motif in *active-Co*.

Transformation of **1-H** in aqueous solution was monitored also by UV-Vis, where a steady increase of the absorbance in the 550 – 600 nm region is registered over the course of 72 h (Figure 6). Indeed, Co(II) aquo-ions do not display any absorption feature in the same spectral window. An analogous UV-Vis spectra variation occurs when **1-H** is aged in 10 mM borate buffer (pH 8), and to a major extent with respect to pure water (inset in figure 6), while no apparent changes are observed in pure acetonitrile. This effect is likely associated to the ability of the solvent to promote ligand dissociation from the Co₄O₄ core, in the order: borate buffer > water > acetonitrile \approx 0.

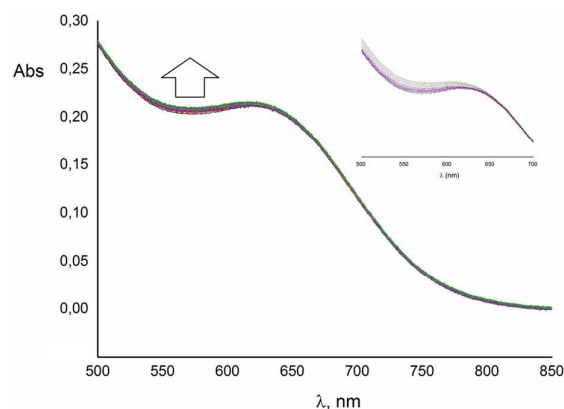


Figure 6. UV-Vis spectra of **1-H** (5 mM in water) over the course of 72 h (1 mm cuvette optical path). Inset: UV-Vis spectra of **1-H** (5 mM in 10 mM borate buffer) over the course of 12 h (1 mm cuvette optical path).

Electrospray ionization mass spectrometry (ESI-MS) was used to get insights into possible ligand dissociation equilibria triggering the cubane evolution into competent WOC. ESI-MS analysis of an aged aqueous solution of **1-H** (figure 7) shows the expected signal at $m/z = 853$ ([HCo₄O₄(CH₃COO)₄(NC₅H₅)₄]⁺), ascribed to protonated **1-H** (protonation of **1-H** is reported in the literature to occur at the oxo-bridges of the Co₄O₄ core, with a pK_a \sim 4).[21] In addition, a second signal at $m/z = 793$ ([Co₄O₄(CH₃COO)₃(NC₅H₅)₄]⁺), is observed, which is attributed to the ion [**1-H**-CH₃COO]⁺, where loss of an acetate bridge from **1-H** is therefore envisaged. In a theoretical, mechanistic study by Siegbahn et al.[24] acetate dissociation was postulated to open a coordination position on the cubane core, thus fostering water coordination as the key step for catalysis. The ESI-MS experimental evidence corroborates this hypothesis as the evolution of the cubane complex to an active WOC is likely to involve the acetate hydrolytic substitution as the primary event of the process.

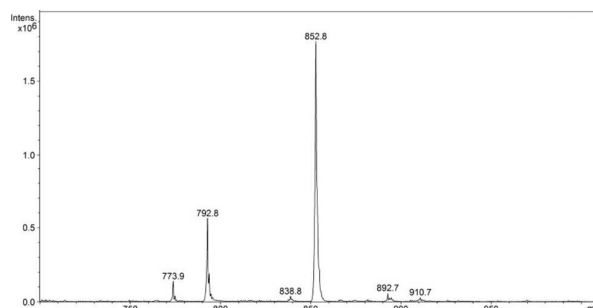


Figure 7. ESI-MS spectra of **1-H** (5×10^{-5} M in acetonitrile, + 0.1% formic acid), aged from a 5 mM solution in 10 mM borate buffer for 21 h.

Behaviour of **1-H** in a photoactivated cycle for water oxidation

The activity of homogeneous catalysts in light driven water oxidation is most commonly investigated in sacrificial systems that take advantage of a photosensitizer and an electron acceptor. Typically, Ru(bpy)₃²⁺ (bpy = 2,2'-bipyridine) is used as the

photosensitizer, while $S_2O_8^{2-}$ (persulfate) is used as the sacrificial electron acceptor. The photocatalytic cycle in the presence of a generic WOC is represented in figure 8, and in equations 2-8.

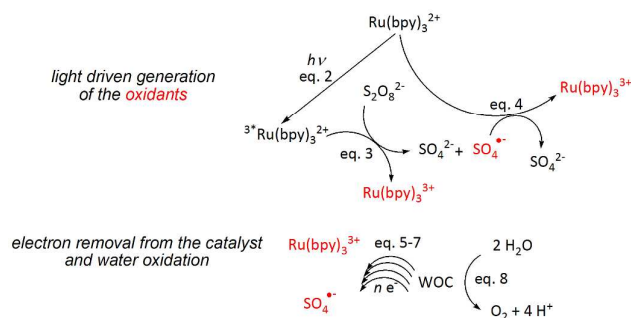
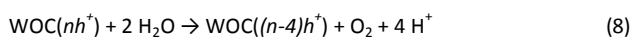
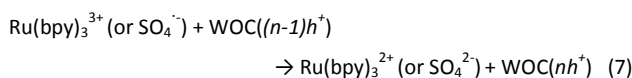
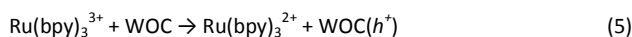
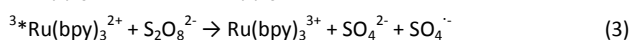


Figure 8. Representation of the processes occurring in a photoactivated water oxidation cycle, with $Ru(bpy)_3^{2+}$ as the photosensitizer, $S_2O_8^{2-}$ as the sacrificial electron acceptor, and a water oxidation catalyst, WOC. The photogenerated oxidants $Ru(bpy)_3^{3+}$ and $SO_4^{\cdot-}$, potentially driving the WOC multi-electron oxidation, are represented in red. See also eqs 2-8.



The first event is light absorption by $Ru(bpy)_3^{2+}$ to generate a triplet manifold ${}^3Ru(bpy)_3^{2+}$ with an energy of ca 2.12 eV (eq. 2),[37] populated in few femtoseconds via intersystem crossing from the singlet.[38] This excited state has a sufficiently long lifetime (ca 500 ns in air equilibrated aqueous solution)[39-40] and reducing ability ($E = -0.84$ vs NHE) to react via a bimolecular route with persulfate (eq. 3), to yield its oxidized form $Ru(bpy)_3^{3+}$ (oxidative quenching), concomitantly with rupture of persulfate O-O bond forming sulfate (SO_4^{2-}) and sulfate radical ($SO_4^{\cdot-}$). Sulfate radical is an extremely strong oxidant (E^0 ca 2.4-3.4 V vs NHE)[30-33] and can abstract one electron from a second $Ru(bpy)_3^{2+}$ molecule to form $Ru(bpy)_3^{3+}$ and SO_4^{2-} (eq. 4). Therefore, from a single photon absorption, two equivalents of $Ru(bpy)_3^{3+}$ can be generated; photogeneration of $Ru(bpy)_3^{3+}$ from $Ru(bpy)_3^{2+}/S_2O_8^{2-}$ is indeed reported to reach a quantum yield of 2 in aqueous solution,[41] indicative of a very efficient process. $Ru(bpy)_3^{3+}$ oxidizes then the WOC to a one-electron oxidised form, generally indicated as $WOC(h^+)$ (eq. 5); alternatively, oxidation of the WOC can be directly promoted by the sulfate radical (eq. 6),[21] a competitive route with respect to reaction 4, where the sulfate radical oxidises $Ru(bpy)_3^{2+}$. If the processes in equations 2-6 described above are repeated several times (at least four), the WOC is oxidized to an active intermediate $WOC(nh^+)$ (eq. 7), capable of oxidizing water to oxygen (eq. 8).

Oxidation of the WOC by sulfate radicals is particularly important to activate WOC operating at high potentials (and thus, not oxidizable directly by $Ru(bpy)_3^{3+}$, $E = 1.26$ vs NHE in aqueous solution), or WOC displaying slow electron transfer kinetics to $Ru(bpy)_3^{3+}$. In the particular case of **1-H** as the WOC, a direct role of persulfate in oxidizing **1-H** was envisaged on the basis of the high operating potential of **1-H**, and on the basis of flash photolysis experiments, that evidenced a progressive reduction of the secondary process in eq. 4, in the presence of increasing aliquots of **1-H**. [21]

In the photocatalytic cycle described in eqs. 2-8, several parameters are important to address the efficiency of the system:

(i) the rate of electron transfer from the WOC to $Ru(bpy)_3^{3+}$ (*hole scavenging*), that is usually characterised by a bimolecular rate constant;[42-45] a high rate of hole scavenging is functional in activating the WOC, but also in preserving the integrity of the photosensitizer, since it limits competitive pathways leading to degradation of $Ru(bpy)_3^{3+}$. [42-45]

(ii) the total amount of oxygen produced, and the derived value of *turnover number (TON)*, given as the ratio of oxygen and the amount of catalyst.

(iii) the maximum rate of oxygen production R_{MAX} , that is then associated to the *turnover frequency (TOF)* of the catalyst, calculated from the ratio of R_{MAX} and the amount of the catalyst.

(iv) the quantum yield for oxygen production (ϕ), defined as the ratio between the amount of oxygen produced and the photons absorbed by the system (eq. 9).

$$\phi = \frac{\text{oxygen produced}}{\text{photons absorbed}} \quad (9)$$

In the $Ru(bpy)_3^{2+}$ / persulfate system, since absorption of one photon can lead to generation of two equivalents of oxidant (either $Ru(bpy)_3^{3+}$ or the sulfate radical), and since four oxidising equivalents are required to oxidise water to oxygen, the theoretical maximum value for the quantum yield is 0.50.[45]

The activity of **1-H** in the photoactivated cycle has been re-evaluated according to these parameters, considering also the aging process of **1-H**, and comparing the results obtained for free Co(II) ions, introduced as Cobalt(II) nitrate, hexahydrate salt.

Electron transfer kinetics (hole scavenging). As anticipated above, one of the crucial step in the light activated cycle, is the electron transfer rate from the catalyst to the oxidized photosensitizer, $Ru(bpy)_3^{3+}$; high electron transfer rates help in preserving the photosensitizer from competitive degradation pathways.[42-45] The electron transfer rates can be determined by nanosecond laser flash photolysis, where a suitable amount of $Ru(bpy)_3^{3+}$ is photo-generated within few ns ($\lambda_{exc} = 355$ nm) according to eqs. 2-4, upon excitation of $Ru(bpy)_3^{2+}$ in the presence of $S_2O_8^{2-}$. Generation of $Ru(bpy)_3^{3+}$ is monitored by a decrease in absorbance (bleaching) of the typical metal-to-ligand-charge-transfer absorption of the $Ru(bpy)_3^{2+}$ at $\lambda = 450$ nm. In the presence of a WOC performing electron transfer to $Ru(bpy)_3^{3+}$, a bleach recovery is observed, indicative of formation of $Ru(bpy)_3^{2+}$, contemporary to the generation of the oxidised form of the WOC (eq. 5). By running the experiment at different concentration of the WOC, and working under pseudo-first-order kinetic conditions ($[WOC] \gg [Ru(bpy)_3^{3+}]$),

a second-order rate constant for the process in eq. 5 can be determined.

As expected, the kinetic traces of $\text{Ru}(\text{bpy})_3^{3+}$ reduction, (Figure 9) obtained with *fresh* **1-H** at different concentrations can be reasonably fitted by means of single-exponential functions, according to eq. 10.

$$[\text{Ru}(\text{bpy})_3^{3+}] = [\text{Ru}(\text{bpy})_3^{3+}]_0 \exp(-k_{\text{obs}} t) + y_0 \quad (10)$$

$$k_{\text{obs}} = k \times [\text{WOC}] \quad (11)$$

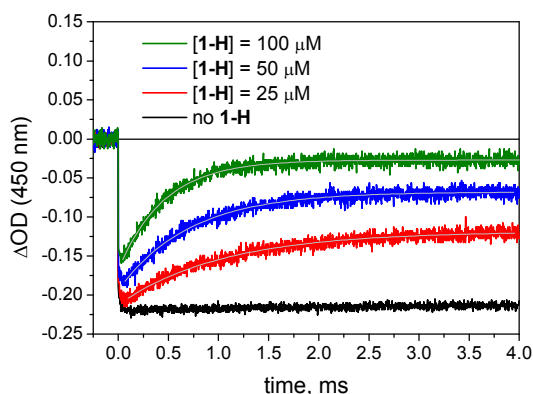


Figure 9. Kinetic traces at 450 nm, with related single-exponential fittings, obtained by laser flash photolysis experiments (excitation at 355 nm, FWHM = 8 ns) on 10 mM borate buffer (pH 8) solutions containing 50 μM $\text{Ru}(\text{bpy})_3^{2+}$, 5 mM $\text{Na}_2\text{S}_2\text{O}_8$, and 0-100 μM **1-H** (from a 5 mM freshly-prepared solution).

Under pseudo-first order kinetic conditions, the pseudo-first order rates k_{obs} can be then divided by the **1-H** concentration, according to eq. 11, and a bimolecular rate constant of $k = 1.7 \times 10^7 \text{ M}^{-1}\text{s}^{-1}$ can be estimated for the electron transfer process from the *fresh* **1-H** to the photogenerated $\text{Ru}(\text{bpy})_3^{3+}$ oxidant in 10 mM borate buffer solutions (pH 8), in perfect agreement with the value obtained previously.[21] The absence of complete recovery of the MLCT bleaching at 450 nm in the presence of **1-H** can be attributed to the poor driving force dictating the electron transfer process ($\Delta G_{\text{ET}} \approx 0$ eV, according to electrochemistry data and without electrostatic correction applied), suggesting that the one-electron oxidation of **1-H** by $\text{Ru}(\text{bpy})_3^{3+}$ could be better described as an equilibrium process rather than an irreversible redox reaction.[21]♣

Interestingly, as shown in Figure 10, evident changes in the $\text{Ru}(\text{bpy})_3^{3+}$ reduction kinetics can be observed in the presence of aged **1-H** (similarly to the CV experiments, **1-H** is aged from a 5 mM stock solution in pure water, and then diluted in 10 mM borate buffer solutions containing the appropriate amounts of $\text{Ru}(\text{bpy})_3^{2+}$ and persulfate). In particular, (i) faster reduction rates are detected with increasing aging time up to 48 h, (ii) the fraction of recovered $\text{Ru}(\text{bpy})_3^{3+}$ increases when the aging time is prolonged, (iii) at both 24 and 48 h aging a single-exponential function is not sufficient to reasonably account for the decay of the $\text{Ru}(\text{bpy})_3^{3+}$ transient species.

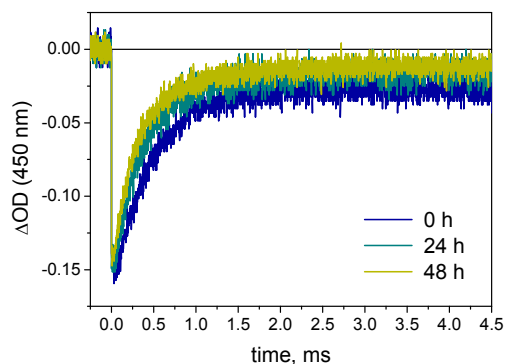


Figure 10. Kinetic traces at 450 nm obtained by laser flash photolysis (excitation at 355 nm, FWHM = 8 ns) on 10 mM borate buffer (pH 8) solutions containing 50 μM $\text{Ru}(\text{bpy})_3^{2+}$, 5 mM $\text{Na}_2\text{S}_2\text{O}_8$, and 100 μM **1-H** at different aging time 0-48 h (from a 5 mM stock solution in water).

All together, these observations are consistent with the evolution of **1-H** in water solution upon aging with formation of *active-Co*, capable of fast hole scavenging from the photogenerated $\text{Ru}(\text{bpy})_3^{3+}$ oxidant. On a more quantitative basis, from the kinetic traces of Figure 10 it is also possible to roughly estimate the bimolecular rate constant of the hole transfer process from $\text{Ru}(\text{bpy})_3^{3+}$ to the *active-Co* species formed upon **1-H** aging. This estimate can be performed by evaluating the difference between the initial rates of $\text{Ru}(\text{bpy})_3^{3+}$ reduction at 0 and 48 h aging and considering 1 μM concentration of *active-Co* formed from a 100 μM total concentration of **1-H** after 48 h aging.¶ This allows to obtain a bimolecular rate constant of $k = 8 \times 10^8 \text{ M}^{-1}\text{s}^{-1}$ for the hole transfer process from the photogenerated $\text{Ru}(\text{bpy})_3^{3+}$ to the *active-Co* species, which is ca. 40-time higher than the bimolecular rate constant of the hole transfer process involving **1-H**. It is worth recalling that free $\text{Co}(\text{II})$ aquo ions give a negligible hole scavenging activity from $\text{Ru}(\text{bpy})_3^{3+}$, under similar conditions on a comparable time window,[44] thus confirming that a different species originates from **1-H** aging in water solution.

Light-driven water oxidation. While hole scavenging kinetics are related to the primary events occurring in the light activated cycle, the actual, oxygenic ability of **1-H** was investigated by continuous irradiation of **1-H** / $\text{Ru}(\text{bpy})_3^{2+}$ / $\text{S}_2\text{O}_8^{2-}$ solutions, simultaneously measuring O_2 formation by means of a fluorescence detector mounted in the headspace of a home-made glass reactor (table 1). The amounts of the photosensitizer $\text{Ru}(\text{bpy})_3^{2+}$ and of the sacrificial electron acceptor $\text{S}_2\text{O}_8^{2-}$ were fixed at 1 mM and 5 mM concentration, respectively,[20-23] while the catalysts were introduced at different concentrations (for **1-H**, the range of the concentration investigated was 18 – 500 μM , entries 1-4 in table 1). The first, clear evidence from the kinetic results, is that when employed at concentrations typically used in experiments of this type,[20-23,46,47] **1-H** displays very poor oxygenic activity (entry 1 in table 1, black trace in figure 12); for the sake of comparison, when $\text{Co}(\text{II})$ is used as the catalyst at the same total Cobalt concentration (being **1-H** a tetrametallic species, a 18 μM concentration of **1-H** corresponds to a total Cobalt concentration of

72 μM), ca 35-fold higher amount of oxygen is produced (entry 6 in table 1, blue trace in figure 12), reaching a notable quantum yield of 0.11.[45] When the concentration of **1-H** is raised (72 - 500 μM , entries 2-4 in table 1, see also red and purple traces in figure 12), a sustained oxygen production is observed. Although the process is subcatalytic, with a formal turnover number per Cobalt centre of up to 0.58 and turnover frequency three orders of magnitudes below literature benchmarks,[20-23,46,47] the system reaches a notable quantum yield of 0.067, when **1-H** is introduced at 180 μM concentration (entry 3 in table 1, purple trace in figure 12).§§

Interestingly, use of aged solutions of **1-H** does not lead to significant changes of the oxygenic performance (entries 4-5 in table 1). Therefore, the presence of *active-Co* (at least in the adopted conditions of entry 5, where it is present in 1% amount with respect to **1-H**) does not lead to net improvements of the oxygenic catalysis, suggesting that under continuous light irradiation, evolution of **1-H** to active intermediates capable of water oxidation occurs rapidly. Indeed, ESI-MS analysis of the reaction mixture in entry 4 in table 1 over the course of photoirradiation, shows the prompt building up of the peak at $m/z = 793$ [**1-H-CH₃COO**]⁺ (Supporting Information), due to loss of an acetate group from the cubane, which was previously observed to initiate the slow, dark evolution of **1-H** in aqueous media, see discussion above.

Table 1. Light driven water oxidation with a WOC/ $\text{Ru}(\text{bpy})_3^{2+}/\text{S}_2\text{O}_8^{2-}$ system. Reactions performed in 15 mL of 10 mM borate buffer, $[\text{Ru}(\text{bpy})_3^{2+}] = 1 \text{ mM}$, $[\text{S}_2\text{O}_8^{2-}] = 5 \text{ mM}$, illumination with a series of six LEDs (total power 42 mW, 7 mW per single LED), corresponding to $9.5 \times 10^{16} \text{ photons s}^{-1}$ ($1.58 \times 10^{-7} \text{ einstein s}^{-1}$) at 450 nm.

#	WOC (conc, μM)	$\mu\text{mol O}_2$ (TON) ^{a,b}	R_{MAX}^c $\mu\text{mol O}_2 \cdot \text{s}^{-1}$ (TOF, s^{-1}) ^{a,c}	ϕ^d
1	1-H fresh (18 μM)	0.15 (0.14)	0.05×10^{-3} (0.04×10^{-3})	
2	1-H fresh (72 μM)	2.50 (0.58)	0.87×10^{-3} (0.20×10^{-3})	
3	1-H fresh (180 μM)	3.30 (0.30)	1.30×10^{-3} (0.11×10^{-3})	0.067
4	1-H fresh (500 μM)	3.60 (0.12)	1.27×10^{-3} (0.042×10^{-3})	
5 ^e	1-H aged 48 h (500 μM)	3.69 (0.12)	1.25×10^{-3} (0.042×10^{-3})	
6	Co(II) (72 μM)	4.60 (4.3)	2.07×10^{-3} (1.92×10^{-3})	0.11

a: for simplicity of interpretation of the data, turnover number (TON) and turnover frequency (TOF) are referred to the total amount of Cobalt introduced. b: determined in the plateau region of the kinetic profile (after 4 h irradiation). c: determined at the maximum slope of the kinetic profile (in the range 10-20 minutes after illumination). d: quantum yield (ϕ) was determined by performing the reaction with illumination with a single LED (7 mW, $2.26 \times 10^{-8} \text{ einstein s}^{-1}$ at 450 nm. e: aged 48 h from 5 mM solution in water.

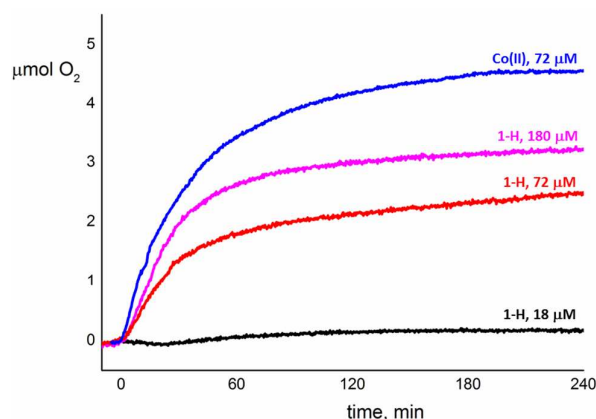


Figure 11. Oxygen evolution kinetics from 15 mL of 10 mM borate buffer, $[\text{Ru}(\text{bpy})_3^{2+}] = 1 \text{ mM}$, $[\text{S}_2\text{O}_8^{2-}] = 5 \text{ mM}$, in the presence of 18, 72, 180 and 500 μM **1-H** (black, red, purple and green traces, respectively) or 72 mM Co(II) (blue trace). Illumination performed with a series of six LEDs (total power 42 mW, 7 mW per single LED), corresponding to $9.5 \times 10^{16} \text{ photons s}^{-1}$ ($1.58 \times 10^{-7} \text{ einstein s}^{-1}$) at 450 nm.

In order to shine light on the building up of the competent intermediates in the **1-H** / $\text{Ru}(\text{bpy})_3^{2+}$ / $\text{S}_2\text{O}_8^{2-}$ three-component system, we followed the photoreaction by continuous-wave EPR. Figure 12a shows the spectral evolution upon irradiation of a solution containing 100 μM **1-H**, 0.5 mM $\text{Ru}(\text{bpy})_3^{2+}$ and $\text{S}_2\text{O}_8^{2-}$ 1.25 mM in 50:50 acetonitrile : 10 mM borate buffer, pH 8. As expected, the initial spectrum, registered for the solution maintained under dark conditions, does not show any significant feature, due to the diamagnetic nature of both **1-H** and of $\text{Ru}(\text{bpy})_3^{2+}$. In the first 10 minutes of illumination (irradiation performed with a series of monochromatic LEDs, emitting at 450 nm), two distinct raising signals are observed. The first one is an axial signal characterised by a $g_{\perp} \sim 2.5$, typical of the Ru(III) form of the photosensitizer,[48] confirming its photogeneration in this system (eqs 2-4). The second signal has an approximately axial line shape, with $g_{\perp} = 2.33$ and $g_{\parallel} = 2.07$ (according to spectral simulations, see Figure 12b); this signal is attributed to the one-electron oxidised form of the cubane, **1-H**⁺, with total electron spin $S=1/2$ and (III,III,III,IV) formal oxidation states for the Cobalt centres, even though the spin is localized over the four metals, thus displaying an average oxidation state $\text{Co}^{+3.25}$. [49] This signal is persistent in the initial period of illumination, and therefore confirms effective oxidation of **1-H** by the photogenerated $\text{Ru}(\text{bpy})_3^{3+}$ (see above discussion). However, after 20 minutes of irradiation, a third, broad signal appears with $g \approx 4.5$ assigned to $S=3/2$ Co(II); this is in line with the formation of Co(II) species,[46,50] likely originated from rearrangement of **1-H**; indeed, its appearance is concomitant to the decrease of the signal of **1-H**⁺. ♦ At first sight, generation of a Co(II) species from **1-H** under oxidising conditions could appear counter-intuitive. However, this Co(II) species could

likely be the resting state of an active species, originated from the cubane, and operating in the light activated cycle.

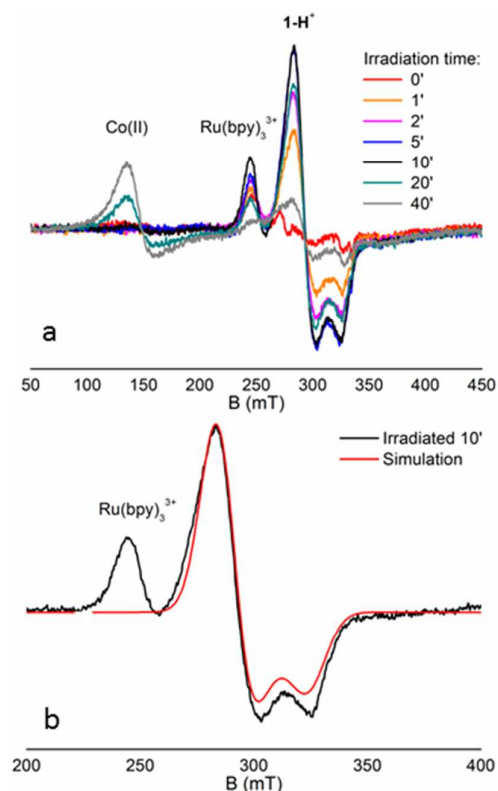


Figure 12. (a) X-band CW-EPR spectra ($T = 10\text{K}$) recorded for **1-H** at different photoirradiation times. (b) X-band CW-EPR spectrum for **1-H** at $10'$ photoirradiation time and corresponding simulation with $g_{\perp} = 2.33$ and $g_{\parallel} = 2.07$. Spectrometer settings are reported in the Experimental Section.

Conclusions

Nowadays, the question whether it is worth designing and spending synthetic efforts for the development of molecular water oxidation catalysts, is a very relevant, open one. In this paper, we have addressed the partial evolution of molecular Co(III) cubanes in aqueous media to an *active-Co* species enabling water oxidation. Several lines of evidence (^{31}P line broadening analysis, UV-Vis spectroscopy, ESI-MS spectrometry) speak against the release of Cobalt aquo-ions by hydrolysis of the cubane, and are instead indicative of a species where the original ligand pool of **1-H** still impacts the catalytic behaviour. In particular, with respect to the pristine **1-H**, *active-Co* shows strongly enhanced electron transfer rate to photogenerated $\text{Ru}(\text{bpy})_3^{3+}$ (*hole scavenging*), with an estimated bimolecular rate constant $8 \times 10^8 \text{ M}^{-1}\text{s}^{-1}$. The hole scavenging rate is one of the parameters where well-defined, molecular species may display superior activity to metal oxide, where in some cases this rate is slow, despite synthetic efforts

to engineer the stabilizing ligand pool.[50] Therefore, the design of molecular species should still be relevant, in order to optimize the interface of the catalyst / photosensitizer modules,[51] within an artificial photosynthetic architecture.

Experimental Section

General methods

Reactions were monitored by analytical thin-layer chromatography (TLC) using silica gel 60 F_{254} pre-coated aluminum sheets and visualized using UV light. Proton NMR spectra were recorded on a Bruker AV300 spectrometers operating at 300 MHz. Proton chemical shifts are reported in parts per million (δ) with the solvent reference relative to tetramethylsilane (TMS) employed as the internal standard (CDCl_3 $\delta = 7.26$ ppm). ^{13}C NMR spectra were recorded on 300 MHz spectrometer operating at 75 MHz with complete proton decoupling. Carbon chemical shifts are reported in parts per million (δ) relative to TMS. UV-Vis kinetic experiments were collected using a Varian Cary-100 Scan spectrophotometer using a 1 mL cell with an optical path length of 1 cm or a 500 μL cell with a length of 1 mm. ESI-MS spectra were recorded on an Agilent 1100 series LC/MSD trap SL spectrometer. Elemental analysis were performed using a *Thermo Scientific Flash 2000* Analyzer.

Starting materials

Cobalt(II) nitrate hexahydrate, sodium acetate trihydrate, hydrogen peroxide solution (30% (w/w) in H_2O), pyridine, 4-methylpyridine, 4-*tert*-butylpyridine, 4-methoxypyridine, 4-pyridinecarbonitrile, 4-bromopyridine hydrochloride, isonicotinic acid, thionyl chloride and triethylamine were obtained commercially as high-purity products and used as received; all solvents were used as received as technical-grade solvents.

Synthesis of isonicotinic acid methyl ester

Thionyl chloride (4.2 mL, 57 mmol) was added to the isonicotinic acid (1.00 g, 8 mmol) under inert atmosphere; the reaction mixture was then heated to reflux and stirred at that temperature for 2h 30 min. The reaction was allowed to cool to room temperature and the residual thionyl chloride was removed under high flux of nitrogen. The resulting solid was dried under vacuum for 2 min, dissolved in methanol (25 mL) at 0°C and triethylamine (1.4 mL, 10 mmol) was added. Subsequently, the reaction was allowed to warm to room temperature and stirred for 18 h. After this time the reaction was quenched with NaHCO_3 s.s. (5 mL) and extracted with dichloromethane (3 x 30 mL). The combined organic solution was dried over dry Na_2SO_4 , filtered and the solvent was removed under reduced pressure. The crude product was purified by flash column chromatography on silica gel with a 95:5 DCM:MeOH mixture as eluent. The purification afforded the desired product in 89% yield. $R_f = 0.73$ (DCM/MeOH 95:5). $^1\text{H-NMR}$ (300 MHz, CDCl_3): δ 8.75 (d, 2H, $J = 4.6$ Hz), 7.81 (d, 2H, $J = 4.6$ Hz), 3.93 (s, 3H).

Synthesis of 1-X

General procedure. Complexes **1-X** were synthesized according to a modified literature procedure.[13] $\text{Co}(\text{NO}_3)_2 \cdot 6\text{H}_2\text{O}$ (2.90 g, 10 mmol) and $\text{CH}_3\text{CO}_2\text{Na} \cdot 3\text{H}_2\text{O}$ (2.70 g, 20 mmol) were dissolved in methanol (30 mL) and heated to refluxing temperature. Properly substituted

pyridine (10 mmol) was then added to the stirred reaction mixture, followed by dropwise addition of an excess of hydrogen peroxide (9.8 M, 4.6 mL, 45 mmol). The reaction mixture was stirred under refluxing condition for 4 h, then allowed to cool to room temperature. The reaction mixture was then diluted with milliQ water (5 mL) and extracted with dichloromethane (150 mL). The organic layer was dried over anhydrous Na₂SO₄, filtered and the solvent was removed under reduced pressure. The crude product was purified by column chromatography with different dichloromethane:methanol mixture as eluent (see below) to afford the pure product.

Co₄(μ₃-O)₄(μ-O₂CMe)₄(NC₅H₅)₄, (1-H). This product was purified by flash column chromatography on silica gel with a 95:5 DCM:MeOH mixture as eluent. The purification afforded the desired product in 54% yield. *R_f* = 0.28 (DCM/MeOH 95:5). ESI-MS (CH₃CN + 0.1% HCOOH; *m/z*): 852.9 [1-H]⁺·H⁺; calcd for [C₂₈H₃₂Co₄N₄O₁₂]⁺·H⁺ 852.9. ¹H-NMR (300 MHz, D₂O): δ 8.20 (d, 8H, *J* = 5.1 Hz), 7.71 (t, 4H, *J* = 7.5 Hz), 7.21 (t, 8H, *J* = 6.6 Hz), 2.07 (s, 12H). ¹³C-NMR (300 MHz, D₂O): δ 189.83, 153.03, 139.93, 125.89, 26.64. Elemental analysis, calcd (%) for C₂₈H₃₂Co₄N₄O₁₂, C 39.46, H 3.78, N 6.57. Found: C 38.83, H 3.92, N 6.05.

Co₄(μ₃-O)₄(μ-O₂CMe)₄(*p*-CH₃NC₅H₄)₄, (1-Me). This product was purified by flash column chromatography on silica gel with a 95:5 DCM:MeOH mixture as eluent. The purification afforded the desired product in 65% yield. *R_f* = 0.27 (DCM/MeOH 95:5). ESI-MS (CH₃CN + 0.1% HCOOH; *m/z*): 909.0 [1-Me]⁺·H⁺; calcd for [C₃₂H₄₀Co₄N₄O₁₂]⁺·H⁺ 909.0. ¹H-NMR (300 MHz, D₂O): δ 7.98 (d, 8H, *J* = 6.3 Hz), 7.06 (d, 8H, *J* = 6.3 Hz), 2.36 (s, 12H), 2.05 (s, 12H). ¹³C-NMR (300 MHz, D₂O): δ 189.71, 152.35, 152.20, 126.71, 26.61, 21.12.

Co₄(μ₃-O)₄(μ-O₂CMe)₄(*p*-C₄H₉NC₅H₄)₄, (1-tBu). This product was purified by flash column chromatography on silica gel with a 98:2 DCM:MeOH mixture as eluent. The purification afforded the desired product in 31% yield. *R_f* = 0.54 (DCM/MeOH 95:5). ESI-MS (CH₃CN + 0.1% HCOOH; *m/z*): 1077.3 [1-tBu]⁺·H⁺; calcd for [C₄₄H₆₄Co₄N₄O₁₂]⁺·H⁺ 1077.2. ¹H-NMR (300 MHz, D₂O): δ 8.16 (d, 8H, *J* = 6.3 Hz), 7.29 (d, 8H, *J* = 6.3 Hz), 2.04 (s, 12H), 1.22 (s, 36H). ¹³C-NMR (300 MHz, D₂O): δ 189.39, 164.52, 152.55, 122.56, 35.32, 30.65, 26.60.

Co₄(μ₃-O)₄(μ-O₂CMe)₄(*p*-OCH₃NC₅H₄)₄, (1-OMe). This product was purified by flash column chromatography on silica gel with a 96:4 DCM:MeOH mixture as eluent. The purification afforded the desired product in 54% yield. *R_f* = 0.37 (DCM/MeOH 95:5). ESI-MS (CH₃CN + 0.1% HCOOH; *m/z*): 973.0 [1-OMe]⁺·H⁺; calcd for [C₃₂H₄₀Co₄N₄O₁₆]⁺·H⁺ 973.0. ¹H-NMR (300 MHz, D₂O): δ 7.97 (d, 8H, *J* = 6.6 Hz), 6.84 (d, 8H, *J* = 6.6 Hz), 3.89 (s, 12H), 2.06 (s, 12H). ¹³C-NMR (300 MHz, D₂O): 189.76, 168.15, 154.03, 112.29, 56.89, 26.59.

Co₄(μ₃-O)₄(μ-O₂CMe)₄(*p*-CN₂NC₅H₄)₄, (1-CN). This product was purified by flash column chromatography on silica gel with a 96:4 DCM:MeOH mixture as eluent. The purification afforded the desired product in 56% yield. *R_f* = 0.63 (DCM/MeOH 95:5). ESI-MS (CH₃CN + 0.1% HCOOH; *m/z*): 952.6 [1-CN]⁺·H⁺; calcd for [C₃₂H₂₈Co₄N₈O₁₂]⁺·H⁺ 952.9. ¹H-NMR (300 MHz, CD₃CN): δ 8.60 (d, 8H, *J* = 5.1 Hz), 7.49 (d, 8H, *J* = 5.1 Hz), 2.02 (s, 12H). ¹³C-NMR (300 MHz, CD₃CN): δ 186.95, 154.72, 126.78, 122.08, 116.72, 26.60.

Co₄(μ₃-O)₄(μ-O₂CMe)₄(*p*-BrNC₅H₄)₄, (1-Br). This product was purified by flash column chromatography on silica gel with a 99:1

DCM:MeOH mixture as eluent. The purification afforded the desired product in 11% yield. *R_f* = 0.24 (DCM/MeOH 99:1). ESI-MS (CH₃CN + 0.1% HCOOH; *m/z*): 1168.6 [1-Br]⁺·H⁺; calcd for [C₂₈H₂₈Br₄Co₄N₄O₁₂]⁺·H⁺ 1164.6 (17%), 1166.6 (68%), 1168.6 (100%), 1169.6 (32%), 1170.6 (67%), 1172.6 (20%). ¹H-NMR (300 MHz, D₂O): δ 8.01 (d, 8H, *J* = 6.0 Hz), 7.56 (d, 8H, *J* = 6.0 Hz), 2.06 (s, 12H). ¹³C-NMR (300 MHz, D₂O): δ 190.13, 153.66, 137.57, 129.54, 26.66.

Co₄(μ₃-O)₄(μ-O₂CMe)₄(*p*-COOCH₃NC₅H₄)₄, (1-COOMe). This product was purified by flash column chromatography on silica gel with a 97:3 DCM:MeOH mixture as eluent. The purification afforded the desired product in 75% yield. *R_f* = 0.24 (DCM/MeOH 97:3). ESI-MS (CH₃CN + 0.1% HCOOH; *m/z*): 1085.0 [1-COOMe]⁺·H⁺; calcd for [C₃₆H₄₀Co₄N₄O₂₀]⁺·H⁺ 1085.0. ¹H-NMR (300 MHz, D₂O): δ 8.41 (d, 8H, *J* = 6.3 Hz), 7.69 (d, 8H, *J* = 6.3 Hz), 3.97 (s, 12H), 2.10 (s, 12H). ¹³C-NMR (300 MHz, D₂O): δ 190.35, 167.04, 154.48, 140.01, 124.74, 54.61, 26.70.

Light-Driven Oxidation of Water. In a typical experiment, 15 mL of a 10 mM borate aqueous buffer containing [Ru(bpy)₃]Cl₂·6H₂O (1 mM), Na₂S₂O₈ (5 mM) and the catalyst were introduced into a glass reactor (internal diameter 18 mm, total internal volume of 24 mL), deoxygenated with nitrogen and allowed to equilibrate at 25 °C under the complete exclusion of light. The solution was then irradiated with a series of six monochromatic LEDs emitting at 450 nm (LED450-06 from Roithner Lasertechnik GmbH). Oxygen evolution was monitored with a FOXY-R-AF probe mounted into the reaction headspace and interfaced with Neoflex Real-Time software for data collection.

Electrochemistry. Cyclic voltammetry experiments were performed using a BAS EC-epsilon potentiostat, in a three-electrode electrochemical cell. Working electrode: Glassy carbon (3 mm diameter, geometric surface area = 7 mm²); counter electrode Pt wire; reference electrode: Ag/AgCl (3 M NaCl); scan rate: 100 mV/s.

Laser flash photolysis. Nanosecond transient measurements were performed with a custom laser spectrometer comprised of a Continuum Surelite II Nd:YAG laser (FWHM 6 - 8 ns) with frequency doubled, (532 nm, 330 mJ) or tripled, (355 nm, 160 mJ) option, an Applied Photophysics xenon light source including a mod. 720 150 W lamp housing, a mod. 620 power controlled lamp supply and a mod. 03-102 arc lamp pulser. Laser excitation was provided at 90° with respect to the white light probe beam. Light transmitted by the sample was focused onto the entrance slit of a 300 mm focal length Acton SpectraPro 2300i triple grating, flat field, double exit monochromator equipped with a photomultiplier detector (Hamamatsu R3896). Signals from the photomultiplier (kinetic traces) were processed by means of a LeCroy 9360 (600 MHz, 5 Gs/s) digital oscilloscope. The white light probe was filtered in order to minimize decomposition of the sample using a band pass filter centered at 450 nm (FWHM = 10 nm).

EPR. X-band continuous-wave EPR spectra were recorded with a Bruker ELEXSYS E580 spectrometer equipped with an ER4102ST cavity operating at 9.38 GHz. Cryogenic temperatures were achieved by using a liquid helium flow cryostat (Oxford Instruments ESR-900) driven by a temperature controller (Oxford Instruments ITC503). The experimental conditions were the following: T = 10 K, non-saturating microwave power: 2 mW, modulation amplitude: 10

G, conversion time: 81.92 ms and time constant:163.84 ms. Simulations of the CW EPR spectra, to obtain the g-tensor principal components, were performed by using the Easyspin routine in Matlab®. g values were estimated by calibration using a sample of strong pitch.

Acknowledgements

We thank Erica Pizzolato for preliminary experiments, Laura Meneghini for registering EPR spectra, Prof. Franco Scandola and Prof. Sebastiano Campagna for fruitful discussions. Financial support from the Italian Ministero dell'Università e della Ricerca (MIUR), (FIRB RBAP11C58Y, "NanoSolar" and PRIN 2010 "Hi-Phuture") and COST actions (CM1205 "CARISMA: CAlytic RoutInes for Small Molecule Activation" and CM1202 "PERSPECT-H2O") are gratefully acknowledged.

Notes and references

⊥ Formation of Co-based WOCs results from the degradation of Co(III) dimers and trimers with a similar ligand pool, induced by bulk electrolysis at anodic potentials.[23] Moreover, active Cobalt-oxide layers are produced by Co aquo ions electrodeposition under anodic scan, and in the presence of proton accepting electrolytes.[18-19]

♠ Reduction potentials of Co(III)/Co(II) couples are reported to be strongly dependent on the ligand pool;[34,35] In particular, pyridine is recognised as a ligand that enhances the reduction potential of the Co(III)/Co(II) couple.[34]

¥ Although this process could occur during the ionization step (since traces of the signal at $m/z = 793$ is observed also in the fresh solution of **1-H**), the higher intensity observed in the spectra of the aged solution of **1-H** speaks in favour of a partial leaching of the carboxylate ligand in aqueous solution, as the primary step of **1-H** decomposition.

♣ A complete recovery of the bleach was instead observed in 50:50 acetonitrile:10 mM borate buffer, pH 8, due to enhanced driving force for the electron transfer.[22] Indeed, this was confirmed to occur for all **1-X** species, with conservation of the Hammett plot of the kinetic constants (see ESI).

¶ Extrapolation of the bimolecular rate constant of the hole transfer process from $\text{Ru}(\text{bpy})_3^{3+}$ to *active-Co* cannot be easily performed by fitting the decay in Figure 11 at 48 h aging due to the complex model to be used for describing the kinetics (i.e., a sum of a pseudo-first order and a second-order kinetics). A rough estimate, however, can be performed as follows: At 48 h aging, the rate R of $\text{Ru}(\text{bpy})_3^{3+}$ reduction is indeed the sum of R_1 and R_2 , where R_1 is the rate of $\text{Ru}(\text{bpy})_3^{3+}$ reduction by **1-H** and R_2 is the rate of $\text{Ru}(\text{bpy})_3^{3+}$ reduction by *active-Co*. Assuming zero-order kinetics in the very beginning of the decays, $R = 0.033 \text{ Ms}^{-1}$ can be calculated as an "initial rate" from the linear fit of the dark yellow trace in Figure 11 between 0 and 200-300 μs , and $R_1 = 0.021 \text{ Ms}^{-1}$ can be calculated as an "initial rate" from the linear fit of the blue trace in Figure 11. The difference $R - R_1$ yields $R_2 = 0.012 \text{ Ms}^{-1}$ with $R_2 = k [\text{Ru}(\text{bpy})_3^{3+}][\text{active-Co}]$, which, considering $[\text{Ru}(\text{bpy})_3^{3+}] = 15 \mu\text{M}$ as the initial concentration of photogenerated oxidant (calculated from ΔOD , $\Delta\epsilon = 13,000 \text{ M}^{-1} \text{ cm}^{-1}$, and the appropriate correction for the ratio between the volume of solution probed by the analyzing beam and that excited by the laser pulse)[43] and $[\text{active-Co}] = 1 \mu\text{M}$ (according to the *active-Co*/[**1-H**] ratio at 48 h aging from EDTA titration), allows to estimate $k = 8 \times 10^8 \text{ M}^{-1} \text{ s}^{-1}$.

§§ Typically, high concentrations of WOC are not used in similar catalytic tests, due to competitive, unproductive quenching of the excited state $^3\text{Ru}(\text{bpy})_3^{2+}$ by the WOC and by its oxidized intermediates, leading to a depletion of the oxygen production and of the quantum yield.[43,46] Conversely, quenching of $^3\text{Ru}(\text{bpy})_3^{2+}$ by **1-H** is negligible.

◆ Cobalt(II) species have been also proposed as precursors for the formation of active cobalt oxide nanoparticles. In this case, analysis of the reaction mixture after 4 h irradiation by Dynamic Light Scattering (DLS) did not show significant scattering.

- [1] S. Berardi, S. Drouet, L. Francàs, C. Gimbert-Suriñach, M. Guttentag, C. Richmond, T. Stoll and A. Llobet, *Chem. Soc. Rev.* **2014**, *43*, 7501.
- [2] (a) K. S. Joya, Y. F. Joya, K. Ocakoglu and R. van de Krol, *Angew. Chem., Int. Ed.* **2013**, *52*, 10426. (b) I. Yasuo, *Coord. Chem. Rev.* **2013**, *257*, 171.
- [3] J. H. Alstrum-Acevedo, M. K. Brennaman and T. J. Meyer, *Inorg. Chem.* **2005**, *44*, 6802.
- [4] C. C. L. McCrory, S. Jung, I. M. Ferrer, S. M. Chatman, J. C. Peters and T. F. Jaramillo, *J. Am. Chem. Soc.* **2015**, *137*, 4347.
- [5] (a) D. G. H. Hetterscheid and L. Sun Eds., cluster issue on water oxidation chemistry, *Eur. J. Inorg. Chem.* **2014**, 568-790. (b) A. Sartorel, M. Carraro, F. M. Toma, M. Prato and M. Bonchio, *En. Env. Sci.* **2012**, *5*, 5592.
- [6] M. D. Kärkäs, O. Verho, E. V. Johnston and B. Åkermark, *Chem. Rev.* **2014**, *114*, 11863.
- [7] K. J. Young, L. A. Martini, R. L. Milot, R. C. Snoberger III, V. S. Batista, C. A. Schmuttenmaer, R. H. Crabtree and G. W. Brudvig, *Coord. Chem. Rev.* **2012**, *256*, 2503.
- [8] X. Sala, S. Maji, R. Bofill, J. Garcia Antón, L. Escriche and A. Llobet, *Acc. Chem. Res.*, **2014**, *47*, 504.
- [9] (a) R. K. Hocking, R. Brimblecome, L. Y. Chang, A. Singh, M. H. Cheah, C. Glover, W. H. Casey and L. Spiccia, *Nat. Chem.* **2011**, *3*, 461. (b) M. M. Najafpour, A. N. Moghaddam, H. Dau and I. Zaharieva, *J. Am. Chem. Soc.* **2014**, *136*, 7245.
- [10] J. J. Stracke and R. G. Finke, *ACS Catalysis* **2014**, *4*, 909.
- [11] S. Fukuzumi and D. C. Hong, *Eur. J. Inorg. Chem.* **2014**, 645.
- [12] V. Artero and M. Fontecave, *Chem. Soc. Rev.* **2013**, *42*, 2338.
- [13] (a) R. Chakrabarty, S. J. Bora and B. K. Das, *Inorg. Chem.* **2007**, *46*, 9450. (b) K. Dimitrou, K. Folting, W. E. Streib and G. Christou, *J. Am. Chem. Soc.* **1993**, *115*, 6432.
- [14] Y. Umena, K. Kawakami, J.-R. Shen and N. Kamiya, *Nature* **2011**, *4*, 55.
- [15] M. Suga, F. Akita, K. Hirata, G. Ueno, H. Murakami, Y. Nakajima, T. Shimizu, K. Yamashita, M. Yamamoto, H. Ago and J.-R. Shen, *Nature* **2015**, *517*, 99.
- [16] M. D. Szymes, Y. Surendranath, D. A. Letterman and D. G. Nocera, *J. Am. Chem. Soc.* **2011**, *133*, 5174.
- [17] M. D. Szymes, D. A. Letterman, T. S. Teets, B. L. Anderson, J. J. Breen, and D. G. Nocera, *ChemSusChem* **2013**, *6*, 65.
- [18] M. W. Kanan and D. G. Nocera, *Science* **2008**, *321*, 1072.
- [19] D. G. Nocera, *Acc. Chem. Res.* **2012**, *45*, 767.
- [20] N. S. McCool, D. M. Robinson, J. E. Sheats and G. C. Dismukes, *J. Am. Chem. Soc.* **2011**, *133*, 11446.
- [21] G. La Ganga, F. Puntoriero, S. Campagna, I. Bazzan, S. Berardi, M. Bonchio, A. Sartorel, M. Natali and F. Scandola, *Faraday Discuss.*, **2012**, *155*, 177.
- [22] S. Berardi, G. La Ganga, M. Natali, I. Bazzan, F. Puntoriero, A. Sartorel, F. Scandola, S. Campagna and M. Bonchio, *J. Am. Chem. Soc.* **2012**, *134*, 11104.

- [23] P. F. Smith, C. Kaplan, J. E. Sheats, D. M. Robinson, N. S. McCool, N. Mezle, G. C. Dismukes, *Inorg Chem*, **2014**, *53*, 2113.
- [24] X. Li and P. E. M. Siegbahn, *J. Am. Chem. Soc.* **2013**, *135*, 13804.
- [25] H.-C. Chen, D. G. H. Hettterscheid, R. M. Williams, J. I. van der Vlugt, J. N. H. Reek and A. M. Brouwer, *Energy Environ. Sci.* **2015**, *8*, 975.
- [26] B. Zhang, F. Li, F. Yu, X. Wang, X. Zhou, H. Li, Y. Jiang and L. Sun, *ACS Catal.* **2014**, *4*, 804.
- [27] G. La Ganga, V. Mollica Nardo, M. Cordaro, M. Natali, S. Vitale, A. Licciardello, F. Nastasi and S. Campagna, *Dalton Trans.* **2014**, *43*, 14926.
- [28] F. Evangelisti, R. Güttinger, R. Moré, S. Lubner and G. R. Patzke, *J. Am. Chem. Soc.* **2013**, *135*, 18734.
- [29] A. M. Ullman, Y. Liu, M. Huynh, D. K. Bediako, H. Wang, B. L. Anderson, D. C. Powers, J. J. Breen, H. D. Abruña, D. G. Nocera, *J. Am. Chem. Soc.* **2014**, *136*, 17681.
- [30] R. Memming, *J. Electrochem. Soc.* **1969**, *116*, 785.
- [31] D. M. Stanbury, A. G. Sykes, in: *Advances in Inorganic Chemistry*; Academic Press: New York, 1989; Vol. 33; pp 69–138.
- [32] A. Lewandoska-Andralojic and D. E. Polyansky, *J. Phys. Chem. A* **2013**, *117*, 10311.
- [33] M. Natali, F. Puntoriero, C. Chiorboli, G. La Ganga, A. Sartorel, M. Bonchio, S. Campagna and F. Scandola, *J. Phys. Chem. C* **2015**, *119*, 2371.
- [34] D. P. Graddon in: *An Introduction to Coordination Chemistry*, Pergamon Press Ltd., Headington Hill Hall, Oxford (UK).
- [35] R. D. Gillard, *J. Chem. Soc. A* **1967**, 917.
- [36] Y. Surendranath, M. W. Kanan and D. G. Nocera, *J. Am. Chem. Soc.* **2012**, *134*, 6326.
- [37] F. Puntoriero, A. Sartorel, M. Orlandi, G. La Ganga, S. Serroni, M. Bonchio, F. Scandola and S. Campagna, *Coord. Chem. Rev.* **2011**, *255*, 2594.
- [38] J. McCusker, *Acc. Chem. Res.* **2003**, *36*, 876.
- [39] (a) A. Juris, V. Balzani, F. Barigelletti, S. Campagna, P. Belser and A. von Zelewsky, *Coord. Chem. Rev.* **1988**, *84*, 85. (b) K. Kalyanasundaram in: *Photochemistry of Polypyridine and Porphyrin Complexes*, Academic, New York, 1992.
- [40] V. Balzani and F. Scandola in: *Supramolecular Photochemistry*, Horwood, Chichester, 1991.
- [41] (a) H. S. White, W. G. Becker and A. J. Bard, *J. Phys. Chem.* **1984**, *88*, 1840. (b) F. Bolletta, A. Juris, M. Maestri and D. Sandrini, *Inorg. Chim. Acta* **1980**, *44*, L175.
- [42] M. Orlandi, R. Argazzi, A. Sartorel, M. Carraro, G. Scorrano, M. Bonchio and F. Scandola, *Chem. Commun.*, **2010**, *46*, 3152.
- [43] M. Natali, M. Orlandi, S. Berardi, S. Campagna, M. Bonchio, A. Sartorel and F. Scandola, *Inorg. Chem.* **2012**, *51*, 7324.
- [44] M. Natali, S. Berardi, A. Sartorel, M. Bonchio, S. Campagna and F. Scandola, *Chem. Commun.* **2012**, *48*, 8808.
- [45] A. Sartorel, M. Bonchio, S. Campagna and F. Scandola, *Chem. Soc. Rev.* **2013**, *42*, 2262.
- [46] E. Pizzolato, M. Natali, B. Posocco, A. Montellano López, I. Bazzan, M. Di Valentin, P. Galloni, V. Conte, M. Bonchio, F. Scandola and A. Sartorel, *Chem. Commun.* **2013**, *49*, 9941.
- [47] (a) H. J. Lv, Y. V. Geletii, C. C. Zhao, J. W. Vickers, G. B. Zhu, Z. Luo, J. Song, T. Q. Lian, D. G. Musaev and C. L. Hill, *Chem. Soc. Rev.* **2012**, *41*, 7572. (b) H. J. Lv, J. Song, Y. V. Geletii, J. W. Vickers, J. M. Sumliner, D. G. Musaev, P. Kogerler, P. F. Zhuk, J. Bacsa, G. B. Zhu and C. L. Hill, *J. Am. Chem. Soc.* **2014**, *136*, 9268.
- [48] A. Volpe, A. Sartorel, C. Tubaro, L. Meneghini, M. Di Valentin, C. Graiff and M. Bonchio, *Eur. J. Inorg. Chem.* **2014**, 665.
- [49] J. G. McAlpin, T. A. Stich, C. A. Ohlin, Y. Surendranath, D. G. Nocera, W. H. Casey and R. D. Britt, *J. Am. Chem. Soc.* **2011**, *133*, 15444.
- [50] W. J. Youngblood, S.-H. A. Lee, Y. Kobayashi, E. A. Hernandez-Pegan, P. G. Hoertz, T. A. Moore, A. L. Moore, D. Gust and T. E. Mallouk, *J. Am. Chem. Soc.* **2009**, *131*, 926.
- [51] A. Montellano López, M. Natali, E. Pizzolato, C. Chiorboli, M. Bonchio, A. Sartorel and F. Scandola, *Phys. Chem. Chem. Phys.* **2014**, *16*, 12000.